Supporting Information

Quinoxaline radical-bridged transition metal complexes with very strong antiferromagnetic coupling

Dimitris I. Alexandropoulos, Kuduva R. Vignesh, Haomiao Xie, and Kim R. Dunbar*

Syntheses

All manipulations were carried out under an inert atmosphere of N_2 using standard Schlenk-line and glovebox techniques unless otherwise noted. The 2,3-di(2-pyridyl)-quinoxaline (dpq) ligand was prepared using literature procedures [1], dried under vacuum, and stored in the glovebox prior to use. The anhydrous MCl_2 (M = Fe, Co, Zn) starting materials were purchased from Sigma Aldrich and stored in an inert atmosphere prior to use. The MeCN solvent was purchased from Sigma Aldrich, purified using an MBRAUN solvent purification system, and stored over fresh molecular sieves in an inert atmosphere prior to use.

Synthesis of $(Cp^*_2Co)[Fe_2Cl_4(dpq)]$ (1). To a stirred pale-yellow solution of $FeCl_2$ (0.051 g, 0.4 mmol) in MeCN (10 mL) was added solid dpq (0.057 g, 0.2 mmol). The dark red mixture was stirred for ~15 min before being combined with a solution of Cp^*_2Co (0.066 g, 0.2 mmol) in MeCN (5 mL). The resulting dark green/brown solution was stirred at room temperature for an additional 10 min and filtered. The filtrate was layered with Et_2O (15 mL) and slow mixing for 2 days yielded dark purple blocks of **1** which were collected by filtration and washed with Et_2O (3 x 5 mL); the yield was 65%. Anal. Calc. for $C_{38}H_{42}Cl_4CoFe_2N_4$ (**1**): C, 52.63; H, 4.88; N, 6.46 %. Found: C, 52.75; H, 4.74; N, 6.32 %. Selected IR data (Nujol mull, cm^{-1}): 1587 (w), 1462 (vs), 1377 (vs), 1351 (w), 1281 (w), 1075 (m), 996 (w), 790 (m), 756 (w), 722 (m), 594 (m), 546 (m).

Synthesis of $(Cp^*_2Co)[Co_2Cl_4(dpq)]$ (2). This compound was prepared in the same manner as **1** but using $CoCl_2$ (0.052 g, 0.4 mmol) in place of $FeCl_2$. After 2 days dark green blocks of **2** had appeared which were collected by filtration and washed with Et_2O (3 x 5 mL); the yield was 75%. Anal. Calc. for $C_{38}H_{42}Cl_4Co_3N_4$ (**2**): C, 52.26; H, 4.85; N, 6.41 %. Found: C, 52.11; H, 4.97; N,

6.29 %. Selected IR data (Nujol mull, cm^{-1}): 1587 (w), 1463 (vs), 1377 (vs), 1305 (m), 1351 (w), 1153 (m), 1078 (w), 1020 (w), 968 (w), 783 (m), 722 (s), 648 (w), 580 (w), 550 (w).

Synthesis of $(Cp^*_2Co)[Zn_2Cl_4(dpq)]$ (3). This compound was prepared in the same manner as **1** but using $ZnCl_2$ (0.055 g, 0.4 mmol) in place of $FeCl_2$. After 2 days dark red blocks of **2** had appeared which were collected by filtration and washed with Et_2O (3 x 5 mL); the yield was 55%. Anal. Calc. for $C_{38}H_{42}Cl_4CoZn_2N_4$ (**3**): C, 51.50; H, 4.78; N, 6.32 %. Found: C, 51.33; H, 4.64; N, 6.45 %. Selected IR data (Nujol mull, cm^{-1}): 1599 (w), 1462 (vs), 1377 (s), 1299 (m), 1208 (w), 1154 (m), 1075 (w), 996 (w), 752 (w), 722 (m), 644 (w), 598 (w), 554 (w).

X-ray Crystallography

Suitable crystals of compounds **1**, **2**, and **3** were selected and mounted on MiTeGen microloops using Paratone oil under ambient conditions. Complete diffraction data for **1** and **3** were collected at 110 K on a Bruker APEXII diffractometer equipped with a MoKα sealed tube source (λ = 0.71073 Å). For compound **2**, complete diffraction data were collected at 110 K on a Bruker D8 VENTURE diffractometer equipped with a multilayer mirror monochromator and a CuKα microfocus sealed tube (λ = 1.54178 Å). For all compounds, the frames were integrated using SAINT+, and absorption effects were corrected by the multi-scan semi-empirical method by SADABS.[2] The structures were solved by the intrinsic phasing methods employed in SHELXT.[3-4] Remaining non-hydrogen atoms were located from the Fourier difference map and refined using SHELXL-2014 using OLEX2[5] as a graphical user interface. All non-hydrogen atoms were successfully refined with anisotropic displacement parameters except when noted in the Crystallographic Refinement Details section below. All hydrogen atoms were placed at calculated positions and refined with riding thermal parameters. The program used for molecular graphics was MERCURY.[6]

Table S1. Crystal data and structural refinement parameters for compounds **1-3**.

Compound	**1**	**2**	**3**
Empirical formula	$C_{38}H_{42}Cl_4CoFe_2N_4$	$C_{38}H_{42}Cl_4Co_3N_4$	$C_{38}H_{42}Cl_4CoZn_2N_4$
Formula weight	867.18	873.34	886.22
Temperature/K	110.0	100.0	110.0
Crystal system	monoclinic	monoclinic	monoclinic
Space group	$P2_1/c$	$P2_1/c$	$P2_1/c$
a/Å	13.440(3)	13.3704(4)	13.302(6)
b/Å	15.842(3)	15.8172(5)	15.821(7)
c/Å	18.607(4)	18.5339(6)	18.600(8)
α/°	90	90	90
β/°	102.501(10)	102.5260(10)	102.662(6)
γ/°	90	90	90
Volume/$Å^3$	3868.0(13)	3826.3(2)	3819(3)
Z	4	4	4
$\rho_{calc}g/cm^3$	1.489	1.516	1.541
μ/mm^{-1}	1.473	12.889	1.988
F(000)	1780.0	1788.0	1812.0
Crystal size/mm^3	0.06 × 0.03 × 0.03	0.1 × 0.05 × 0.04	0.04 × 0.02 × 0.02
Radiation	MoKα (λ = 0.71073)	CuKα (λ = 1.54178)	MoKα (λ = 0.71073)
2Θ range for data collection/°	4.274 to 51.72	6.772 to 137.468	4.06 to 52.034
Index ranges	$-16 \le h \le 16$ $-19 \le k \le 19$ $-22 \le l \le 22$	$-16 \le h \le 16$, $-19 \le k \le 19$, $-22 \le l \le 22$	$-16 \le h \le 16$ $-19 \le k \le 19$ $-22 \le l \le 22$
Reflections collected	141519	56580	53412
Independent reflections	7441 $R_{int} = 0.0398$	7068 $R_{int} = 0.0706$	7083 $R_{int} = 0.1027$

	R_{sigma} = 0.0140	R_{sigma} = 0.0377	R_{sigma} = 0.0634
Data / restraints / parameters	7441 / 0 / 452	7068 / 0 / 452	7083 / 0 / 452
Goodness-of-fit on F_2	1.041	1.051	1.065
Final $R_{a,b}$ indexes [I>=2σ (I)]	R_1 = 0.0271 wR_2 = 0.0666	R_1 = 0.0505 wR_2 = 0.1133	R_1 = 0.0582 wR_2 = 0.1442
Final $R_{a,b}$ indexes [all data]	R_1 = 0.0309 wR_2 = 0.0692	R_1 = 0.0588 wR_2 = 0.1207	R_1 = 0.0841 wR_2 = 0.1676
Largest diff. peak / hole / e Å^{-3}	1.05 / -0.64	0.92 / -0.86	1.45 / -1.32

$^a R_1 = \Sigma(||F_o| - |F_c||)/\Sigma|F_o|$. $^b wR_2 = [\Sigma[w(F_{o2} - F_{c2})_2]/\Sigma[w(F_{o2})_2]]_{1/2}$, $w = 1/[\sigma_2(F_{o2}) + (ap)_2 + bp]$, where $p = [\max(F_{o2}, 0) + 2F_{c2}]/3$.

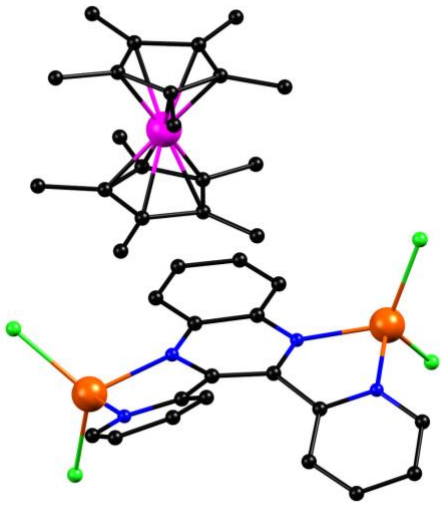

Figure S1. Asymmetric unit of **1**. Colors: Fe$_{II}$, orange; N, blue; C, black. Hydrogen atoms are omitted for the sake of clarity.

Table S1. Selected distances and angles for compounds **1**-**3**.

Compound **1**			
Bond lengths (Å)			
Fe(1)-Cl(1)	2.2372(6)	Fe(2)-N(4)	2.0801(2)
Fe(1)-Cl(2)	2.2545(6)	**N(1)-C(6)**	**1.386(2)**
Fe(1)-N(1)	2.0431(2)	**N(1)-C(7)**	**1.363(2)**
Fe(1)-N(2)	2.0989(2)	**N(2)-C(1)**	**1.381(2)**
Fe(2)-Cl(3)	2.2483(5)	**N(2)-C(8)**	**1.367(2)**
Fe(2)-Cl(4)	2.2615(8)	**C(1)-C(6)**	**1.412(3)**
Fe(2)-N(2)	2.0418(2)	**C(7)-C(8)**	**1.397(3)**
Bond angles (°)			
Cl(1)-Fe(1)-Cl(2)	113.98(3)	Cl(3)-Fe(2)-Cl(4)	120.52(3)
N(1)-Fe(1)-Cl(1)	113.76(5)	N(2)-Fe(2)-Cl(3)	117.64(5)
N(1)-Fe(1)-Cl(2)	117.24(5)	N(2)-Fe(2)-Cl(4)	111.32(5)
N(1)-Fe(1)-N(3)	77.88(6)	N(2)-Fe(2)-N(4)	77.68(6)
N(3)-Fe(1)-Cl(1)	116.28(5)	N(4)-Fe(2)-Cl(3)	109.27(5)
N(3)-Fe(1)-Cl(2)	113.04(5)	N(4)-Fe(2)-Cl(4)	112.37(5)
Compound **2**			
Bond lengths (Å)			
Co(1)-Cl(1)	2.2229(1)	Co(2)-N(4)	2.026(3)

Co(1)-Cl(2)	2.2380(1)	**N(1)-C(6)**	**1.387(5)**
Co(1)-N(1)	1.970(3)	**N(1)-C(7)**	**1.366(5)**
Co(1)-N(2)	2.040(3)	**N(2)-C(1)**	**1.393(5)**
Co(2)-Cl(3)	2.2360(1)	**N(2)-C(8)**	**1.366(5)**
Co(2)-Cl(4)	2.2394(1)	**C(1)-C(6)**	**1.399(5)**
Co(2)-N(2)	1.962(3)	**C(7)-C(8)**	**1.395(5)**
Bond angles (°)			
Cl(1)-Co(1)-Cl(2)	110.21(4)	Cl(3)-Co(2)-Cl(4)	116.53(5)
N(1)-Co(1)-Cl(1)	115.67(1)	N(2)-Co(2)-Cl(3)	120.48(1)
N(1)-Co(1)-Cl(2)	118.67(1)	N(2)-Co(2)-Cl(4)	112.75(1)
N(1)-Co(1)-N(3)	81.17(1)	N(2)-Co(2)-N(4)	80.91(1)
N(3)-Co(1)-Cl(1)	115.04(1)	N(4)-Co(2)-Cl(3)	108.52(1)
N(3)-Co(1)-Cl(2)	113.46(1)	N(4)-Co(2)-Cl(4)	111.69(1)
Compound **3**			
Bond lengths (Å)			
Zn(1)-Cl(1)	2.1958(2)	Zn(2)-N(4)	2.029(4)
Zn(1)-Cl(2)	2.2224(1)	**N(1)-C(6)**	**1.363(6)**
Zn(1)-N(1)	2.023(4)	**N(1)-C(7)**	**1.356(6)**
Zn(1)-N(2)	2.049(4)	**N(2)-C(1)**	**1.377(6)**
Zn(2)-Cl(3)	2.2192(2)	**N(2)-C(8)**	**1.362(6)**

Zn(2)-Cl(4)	2.2211(2)	**C(1)-C(6)**	**1.415(6)**
Zn(2)-N(2)	2.020(4)	**C(7)-C(8)**	**1.401(6)**
Bond angles (°)			
Cl(1)-Zn(1)-Cl(2)	112.98(6)	Cl(3)-Zn(2)-Cl(4)	117.73(6)
N(1)-Zn(1)-Cl(1)	115.21(1)	N(2)-Zn(2)-Cl(3)	116.94(1)
N(1)-Zn(1)-Cl(2)	115.55(12)	N(2)-Zn(2)-Cl(4)	112.93(1)
N(1)-Zn(1)-N(3)	80.34(2)	N(2)-Zn(2)-N(4)	80.12(6)
N(3)-Zn(1)-Cl(1)	114.97(1)	N(4)-Zn(2)-Cl(3)	110.05(1)
N(3)-Zn(1)-Cl(2)	114.07(1)	N(4)-Zn(2)-Cl(4)	113.09(1)

BVS calculations

Table S3. Bond valence sum (BVS) calculations for Co and Fe atoms in **1** and **2**, respectively.

Compound **1**			Compound **2**		
Atom	Co^{II}	Co^{III}	Atom	Fe^{II}	Fe^{III}
Co1	2.03	2.09	Fe1	2.08	2.35
Co2	2.04	2.09	Fe2	2.09	2.35

Cyclic voltammetry

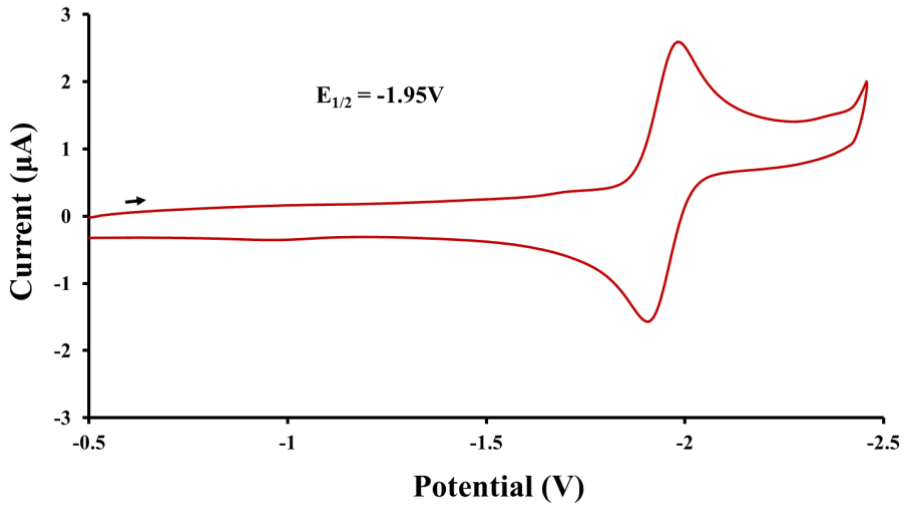

Figure S2. Cyclic voltammogram at 100 mV s^{-1} for the dpq ligand in MeCN containing 0.1 M $NBu^{n}_{4}PF_6$ as the supporting electrolyte. The indicated potentials are *vs* Fc/Fc^{+}.

Magnetism

Variable-temperature direct current (dc) magnetic susceptibility data were collected on a Quantum Design MPMS-XL SQUID magnetometer equipped with a 7 T magnet and operating in the 2.0-300 K range. Microcrystalline samples were packed in a polypropylene bag in order to avoid torquing of the crystallites. The diamagnetic contribution of the polypropylene bag used to hold the sample was subtracted from the raw data. Pascal's[7] constants were used to estimate the diamagnetic corrections, which were subtracted from the experimental susceptibilities to give the molar paramagnetic susceptibilities (χ_M). Reduced magnetization data were collected from 2 K to 5 K (with 0.2 K steps) at magnetic fields ranging from 1 T to 7 T.

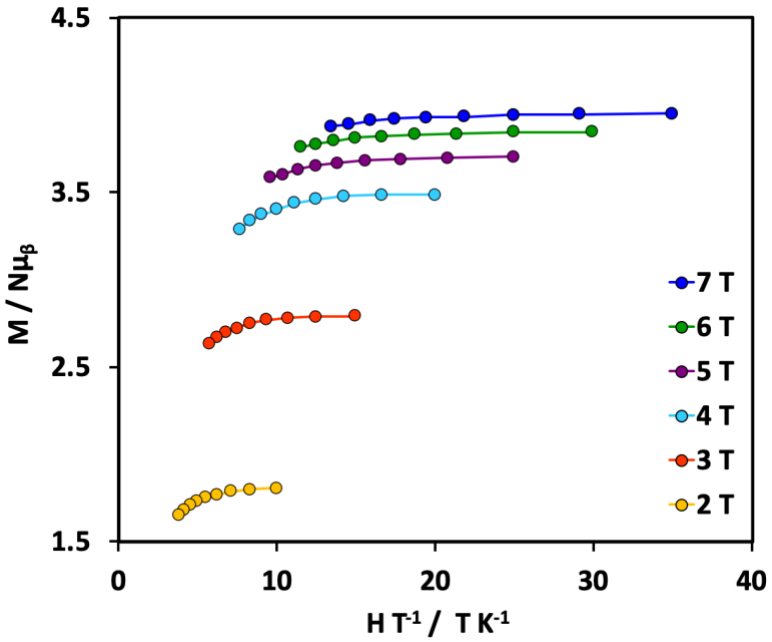

Figure S3. Reduced magnetization data for **1**. Solid lines are guides for the eye.

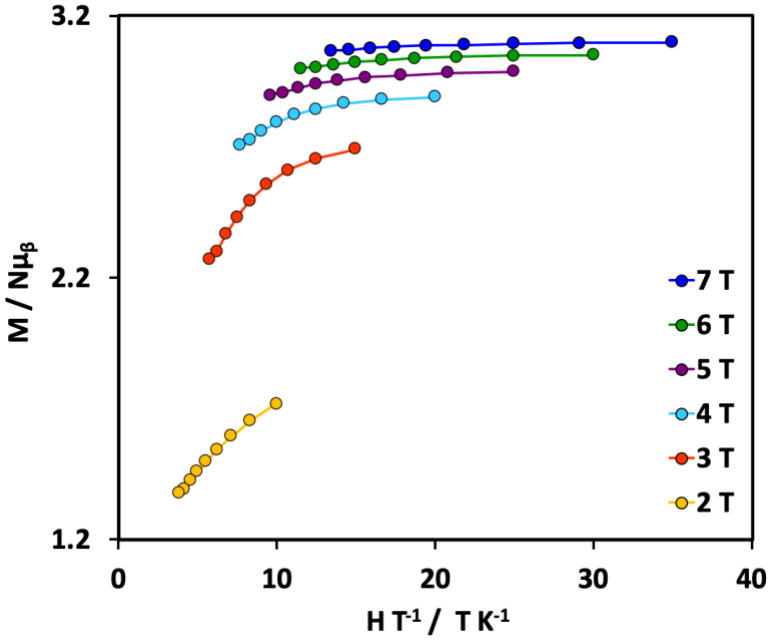

Figure S4. Reduced magnetization data for **2**. Solid lines are guides for the eye.

Computational details

DFT calculations: We employed B3LYP[8] functionals with Ahlrichs[9] triple- ζ basis set as implemented in the Gaussian 09[10] suite of programs to calculate the energies of the three spin states of **1** and **2** (Table S4). The *J* values were computed from the energy differences between the high spin (E_{HS}) state calculated using single determinant wave functions, and the low spin (E_{BS}) state determined using the Broken Symmetry (BS) approach developed by Noodleman.[11] The BS approach has a proven record of yielding good numerical estimates of *J* constants for a variety of complexes,[12] especially radical complexes.[13]

Table S4. Energy of the spin states produced by DFT calculations for complex **1**.

Spin State, S	For single-point calculation using crystal structure	
	E_S (Hartree)	$\Delta E = E_S - E_{9/2}$ (cm^{-1})
9/2	-5280.72371751	0
7/2	-5280.73393590	-2242.7
1/2	-5280.72863872	-1080.1

Table S5. Energy of the spin states produced by DFT calculations for complex **2**.

Spin State, S	For single-point calculation using crystal structure	
	E_S (Hartree)	$\Delta E = E_S - E_{7/2}$ (cm^{-1})
7/2	-5518.902204670	0
5/2	-5518.911038800	-1938.9
1/2	-5518.906493100	-941.2

In the case of a two spin system and using the spin Hamiltonian $\mathbf{H = -2J_{ij}S_iS_j}$, the energy difference between the high spin and low spin state is:

$E_{HS} - E_{BS} = -4J_{ij}S_iS_j$

Considerations related to the self-interaction error in commonly used exchange functional, non-dynamic pair correlation effects, and the application of spin projection techniques to DFT calculations led to the following equation to describe the energy difference:

$E_{HSDFT} - E_{BSDFT} = -4J_{ij}(S_iS_j + S_j)$, where $S_i > S_j$.

Application of this formalism to the three-spin system of complex **1** that consists of two Fe^{2+} ions bridged by the dpq radical ligand, leads to the following expressions for the differences between the energies for the three spin states calculated by DFT methods:

$$E_{7/2} - E_{9/2} = 10J_{Fe-rad}$$

$$E_{1/2} - E_{9/2} = 20J_{Fe-Fe} + 5J_{Fe-rad}$$

$$J_{Fe-rad} = \frac{1}{10}(-2242.7\ cm^{-1}) = -224.3\ cm^{-1}$$

$$J_{Fe-Fe} = \frac{1}{20}\ ((-5 * -224.3\ cm^{-1}) - 1080.1\ cm^{-1}) =\ 2.1\ cm^{-1}$$

Similarly, for complex **2** that consists of two Co^{2+} ions bridged by the dbq radical ligand,

$$E_{5/2} - E_{7/2} = 8J_{Co-rad}$$

$$E_{1/2} - E_{7/2} = 12J_{Co-Co} + 4J_{Co-rad}$$

$$J_{Co-rad} = \frac{1}{8}(-1938.9\ cm^{-1}) = -242.4\ cm^{-1}$$

$$J_{Co-Co} = \frac{1}{12}\ ((-4 * -242.4\ cm^{-1}) - 941.2\ cm^{-1}) =\ 2.4\ cm^{-1}$$

***Ab initio* Calculations:** We performed *ab initio* calculations based on the wave function theory approach to compute the ZFS of both Fe^{II} and Co^{II} ions in **1** and **2**, respectively using ORCA 3.0 programme.[14] We employed BP86 functional along with scalar relativistic ZORA Hamiltonian and ZORA-def2-TZVP basis sets for the metal ions and the first coordination sphere atoms and ZORA-def2-SVP was used for the remaining atoms. The RI approximation with secondary TZV/*J* Columbic fitting basis sets were used along with increased integration grids (Grid 5 in ORCA convention). The tight SCF convergence was used throughout the calculations ($1x10^{-8}$ Eh). The SOC contributions in the *ab initio* framework were obtained using second-order perturbation theory as well as employing the effective Hamiltonian approach which enables calculations of all matrix elements to be made of the anisotropic spin Hamiltonian from the *ab initio* energies and wave functions numerically. Here we employed the state average-CASSCF (Complete Active Space Self-Consistent Field) method to compute the ZFS. The active space comprises of six active electrons in five active d-orbitals (d_6 system; CAS (6,5)) for Fe^{II} ion and seven active electrons in five active d-orbitals (d_7 system; CAS (7,5)) for Co^{II} ion. With this active space, we computed all of the 5 quintet and 45 triplet states for Fe^{II} ion, 10 quartet and 40 doublet states for Co^{II} ion in the configuration interaction procedure.[15] The d-orbital ordering was plotted using 'LOEWDIN-energies' from the ORCA output that contains each root contribution and the corresponding electronic arrangement along with their plausible transition energies. The Effective Hamiltonian from the CASSCF calculation provides the calculated D and E parameters with their "Individual contribution to the D-tensor". For each contribution the program predicts the plausible transition energies between the d-orbitals and those D values compared with the LOEWDIN energies.

Table S6. CASSCF computed energies (cm^{-1}) and contributions to *D* value of a Fe^{II} ion in **1** and a Co^{II} ion in **2** from first four quintet and quartet excited states, respectively.

Complex	Excited state	Energy	*D* Contribution
1	First	1707.2	5.0
	Second	4313.0	0.6
	Third	5668.2	0.1
	Fourth	6784.7	1.8
2	First	1853.8	15.0
	Second	2211.4	22.4
	Third	3099.1	-17.6
	Fourth	5385.6	6.5

References:

1. Goodwin, H. A.; Lions, F., Tridentate Chelate Compounds. II1. *J. Am. Chem. Soc.* **1959,** *81* (24), 6415-6422.

2. Sheldrick, G. M., Program for Empirical Absorption Correction of Area Detector Data. *SADABS* **1996**.

3. Sheldrick, G., SHELXT - Integrated space-group and crystal-structure determination. *Acta Cryst. Sec. A* **2015,** *71* (1), 3-8.

4. Sheldrick, G., Crystal structure refinement with SHELXL. *Acta Cryst. Sec. C* **2015,** *71* (1), 3-8.

5. Dolomanov, O. V.; Bourhis, L. J.; Gildea, R. J.; Howard, J. A. K.; Puschmann, H., OLEX2: a complete structure solution, refinement and analysis program. *J. Appl. Cryst.* **2009,** *42* (2), 339-341.

6. Macrae, C. F.; Edgington, P. R.; McCabe, P.; Pidcock, E.; Shields, G. P.; Taylor, R.; Towler, M.; van de Streek, J., Mercury: visualization and analysis of crystal structures. *J. Appl. Cryst.* **2006,** *39* (3), 453-457.

7. Bain, G. A.; Berry, J. F., Diamagnetic Corrections and Pascal's Constants. *J. Chem. Educ.* **2008,** *85* (4), 532.

8. A. D.Becke, *J. Chem. Phys.* **1993,** *98*, 5648-5652.

9. (a) A. Schaefer, H. Horn, R. Ahlrichs, *J. Chem. Phys.* **1992,** *97*, 2571-2577; (b) A.Schaefer, C.Huber, R. Ahlrichs, *J. Chem. Phys.* **1994,** *100*, 5829-5835.

10. M. J. Frisch, G. W. Trucks, H. B. Schlegel, G. E. Scuseria, M. A. Robb, J. R. Cheeseman, G. Scalmani, V. Barone, B. Mennucci, G. A. Petersson, H. Nakatsuji, M. Caricato, X. Li, H. P. Hratchian, A. F. Izmaylov, J. Bloino, G. Zheng, J. L. Sonnenberg, M. Hada, M. Ehara, K. Toyota, R. Fukuda, J. Hasegawa, M. Ishida, T. Nakajima, Y. Honda, O. Kitao, H. Nakai, T. Vreven, J. A. Montgomery, J. E. Peralta, F. Ogliaro, M. Bearpark, J. J. Heyd, E. Brothers, K. N. Kudin, V. N. Staroverov, R. Kobayashi, J. Normand, K. Raghavachari, A. Rendell, J. C. Burant, S. S. Iyengar, J. Tomasi, M. Cossi, N. Rega, J. M. Millam, M. Klene, J. E. Knox, J. B. Cross, V. Bakken, C. Adamo, J. Jaramillo, R. Gomperts, R. E. Stratmann, O. Yazyev, A. J. Austin, R. Cammi, C. Pomelli, J. W. Ochterski, R. L. Martin, K. Morokuma, V. G. Zakrzewski, G. A. Voth, P. Salvador, J. J. Dannenberg, S. Dapprich, A. D. Daniels, Ö. Farkas, J. B. Foresman, J. V. Ortiz, A. J. Cioslowski, D. J. Fox and I. Gaussian, Gaussian 09 (Revision A.02), Wallingford CT, 2009.

11. L. Noodleman, , *J. Chem. Phys.* **1981,** *74*, 5737-5743.

12. (a) S. Piligkos, G. Rajaraman, M. Soler, N. Kirchner, J. van Slageren, R. Bircher, S. Parsons, H.-U. Gudel, J. Kortus, W. Wernsdorfer, G. Christou and E. K. Brechin, *J. Am. Chem. Soc.*, **2005**, *127*, 5572–5580. (b) G. Rajaraman, J. Cano, E. K. Brechin and E. J. L. McInnes, *Chem. Commun.*, **2004**, 1476–1477. (c) E. Ruiz, J. Cano, S. Alvarez and P. Alemany, *J. Comput. Chem.*, **1999**, *20*, 1391–1400. (d) K. R. Vignesh, S. K. Langley, K. S. Murray and G. Rajaraman, *Chem. – Eur. J.*, **2015**, *21*, 2881–2892.

13. (a) I. A. Gass, S. Tewary, A. Nafady, N. F. Chilton, C. J. Gartshore, M. Asadi, D.W. Lupton, B. Moubaraki, A. M. Bond, J. F.Boas, S.-X. Guo, G. Rajaraman, K. S. Murray, *Inorg. Chem.* **2013,** *52*, 7557-7572; (b) T. Rajeshkumar, G. Rajaraman, *Chem. Commun.* **2012,** *48*, 7856-7858. (c) D. I. Alexandropoulos, B. S. Dolinar, K. R. Vignesh and K. R. Dunbar, *J. Am. Chem. Soc.*, 2017, **139**, 11040-11043;

14. F. Neese, The ORCA program system. *WIRES: Comput. Mol. Sci.* **2012,** *2* (1), 73-78.

15. F. Weigend, R.Ahlrichs, *Phys. Chem. Chem. Phys.* **2005,** *7* (18), 3297-3305.